2017

Structure of the N-glycans from the chlorovirus NE-JV-1

Immacolata Speciale
University of Napoli, immacolata.speciale@unina.it

Irina Agarkova
University of Nebraska-Lincoln, iagarkova2@unl.edu

Garry Duncan
Nebraska Wesleyan University, gduncan@nebrwesleyan.edu

James L. Van Etten
University of Nebraska-Lincoln, jvanetten1@unl.edu

Cristina De Castro
University of Napoli, decastro@unina.it

Structure of the N-glycans from the chlorovirus NE-JV-1

Immacolata Speciale, Irina Agarkova, Garry A. Duncan, James L. Van Etten, & Cristina De Castro

I. Speciale (*Corresponding author*), Department of Chemical Sciences, University of Napoli, 80126 Naples, Italy; *email* immacolata.speciale@unina.it

C. De Castro, Department of Agricultural Sciences, University of Napoli, 80055 Portici, Italy

I. Agarkova & **J. L. Van Etten**, Department of Plant Pathology and Nebraska Center for Virology, University of Nebraska, Lincoln, NE 68583-0900, USA

G. A. Duncan, Department of Biology, Nebraska Wesleyan University, Lincoln, NE, USA

Abstract

Results from recent studies are breaking the paradigm that all viruses depend on their host machinery to glycosylate their proteins. Chloroviruses encode several genes involved in glycan biosynthesis and some of their capsid proteins are decorated with N-linked oligosaccharides with unique features. Here we describe the elucidation of the N-glycan structure of an unusual chlorovirus, NE-JV-1, that belongs to the Pbi group. The host for NE-JV-1 is the zoochlorella *Micractinium conductrix.* Spectroscopic analyses established that this N-glycan consists of a core region that is conserved in all of the chloroviruses. The one difference is that the residue 3OMe-L-rhamnose is acetylated at the O-2 position in a non-stoichiometric fashion.

Keywords — *Chlorovirus, Micractinium conductrix,* Pbi virus, Virus NE-JV-1, NMR analysis

Published in *Antonie van Leeuwenhoek* 110 (2017), pp 1391–1399.
DOI 10.1007/s10482-017-0861-3
Submitted 12 January 2017; accepted 14 March 2017; published 22 March 2017.

Introduction

Chloroviruses (family *Phycodnaviridae*) infect unicellular, eukaryotic, symbiotic chlorella-like green algae, also called zoochlorellae, which establish symbiotic relationships with the protozoan *Paramecium bursaria*, the coelenterate *Hydra viridis*, and the heliozoan *Acanthocystis turfacea* (Van Etten and Dunigan 2012, 2016). Zoochlorellae are resistant to viruses in their symbiotic state, but the algae can grow independently from their hosts in the laboratory and thus one can study the virus-algal relationships. Viruses that infect zoochlorellae are classified into four groups depending on their hosts: NC64A viruses that infect *Chlorella variabilis* strain NC64A, Syn viruses that infect *C. variabilis* strain Syngen, SAG viruses that infect *Chlorella heliozoae* strain 3.83; and Pbi viruses that infect *Micractinium conductrix* strain Pbi (Quispe et al. 2016; Van Etten et al. 2010).

Chloroviruses are large, icosahedral, plaque forming, dsDNA viruses (Yamada et al. 2006; Van Etten and Dunigan 2012, 2016). One important characteristic of these viruses is that they encode most, if not all, of the components required to glycosylate their major capsid proteins (Van Etten et al. 2010). This characteristic differs from other viruses infecting eukaryotic organisms that use the host biosynthetic machinery (e.g., Doms et al. 1993; Olofsson and Hansen 1998; Vigerust and Shepherd 2007). Recently the N-glycan structure(s) of several chloroviruses have been reported and they showed a conserved core motif that does not resemble any other reported structure in bacteria, archaea or eukarya (De Castro et al. 2016). This conserved core structure consists of five monosaccharides (**Fig. 1a**), β-D-glucose is at the reducing end and it is attached to the protein via a N-glycosidic linkage, β-D-xylose and α-D-fucose elongate this first residue at O-4 and O-3, respectively. This xylose is referred to as the proximal xylose because it is the closest of the two xyloses to the protein backbone. The two residues attached to fucose are: α-D-galactose at O-2 and the distal β-D-xylose at O-4, respectively. The remaining fucose position O-3 is substituted with a semiconserved element, an α-rhamnose, the configuration of which depends on the group to which the chlorovirus belongs; for instance, it is in the D form in the NC64A and Syn viruses and in the L form in the Pbi and SAG viruses. Also, the L-rhamnose residue is methylated at O-3 in the Pbi and SAG viruses. Different chloroviruses present this conserved core motif

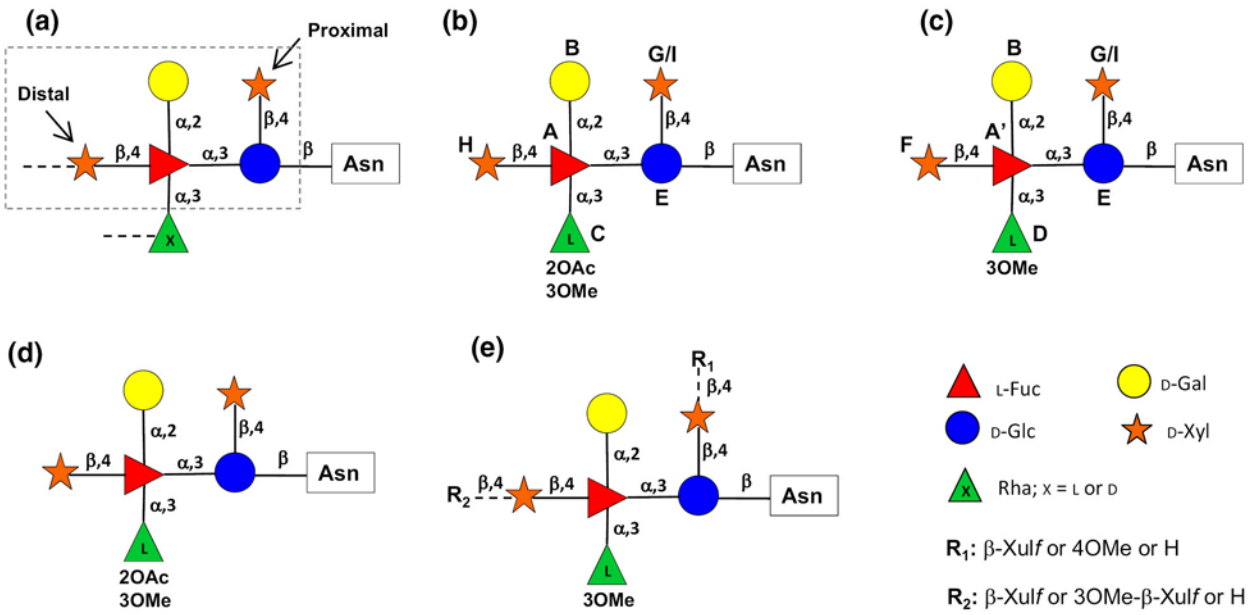

Fig. 1. Structures of different chlorovirus N-glycans. **a)** The conserved core motif is enclosed in the *grey dotted box*, while the residue outside the box is the semi-conserved element. **b)** The acetylated glycoform from virus NE-JV-1; the residues are labelled with the *letter* used during NMR analysis. **c)** second glycoform isolated from NE-JV-1, of note this structure was described also for ATCV-1 N-glycan. **d**, **e)** N-glycans from Pbi chlorovirus CVM-1, and MT325, respectively. Xul*f* is xylulofuranose. Structure of N-glycans from ATCV-1, MT325 and CVM-1 are adapted from De Castro et al. 2016.

and modify it further by the addition of other decorations, either monosaccharides or acetyls or methyl, so that the final N-glycan is unique and represents the signature of a specific virus (De Castro et al. 2016).

Forty-one chlorovirus genomes, representing NC64A, SAG, and Pbi viruses, have been sequenced and phylogenetic relationships were determined using 32 concatenated proteins encoded by all of the viruses (Jeanniard et al. 2013). This analysis showed that viruses infecting the same algal host cluster into monophyletic clades. One exception to this scenario was virus NE-JV-1, which appeared as a sole member of a subgroup of Pbi viruses. NE-JV-1 shares 74% amino acid identity on average with the other Pbi viruses in the 32 core proteins used in the phylogenic reconstruction. For comparison, the within-clade average protein amino acid identity was 93, 95, and 97% for NC64A, SAG and Pbi (excluding NE-JV-1) viruses, respectively. Between clades, the protein sequence identity ranged from 63% (NC64A vs. Pbi viruses) to 71% (Pbi vs. SAG viruses).

Virus NE-JV-1, like the other Pbi viruses, also lacks the genes needed to synthesize L-fucose and D-rhamnose-activated precursors; these genes are common in the other chloroviruses and the two sugars are present in some of their capsid protein N-glycans. These NE-JV-1 properties prompted us to examine the N-glycan structure(s) of the NE-JV-1 major capsid glycoprotein.

Materials and methods

Glycopeptide isolation

Isolation of the major capsid protein from NE-JV-1 was performed by suspending the virus (1 ml, ~10^{11} plaque forming units) in phosphate-buffered saline (PBS) and heating the solution at 70 °C for 20 min. After cooling, the solution was centrifuged (11.49*g*, 4 °C, 30 min) and the major capsid protein was precipitated from the clear supernatant by adding four volumes of cold acetone. The protein, which appeared as a single band on SDS-PAGE (**Fig. 2**), was recovered by centrifugation as above, suspended in water and lyophilized (~1 mg). Glycopeptides were isolated from the major capsid protein by enzymatic hydrolysis

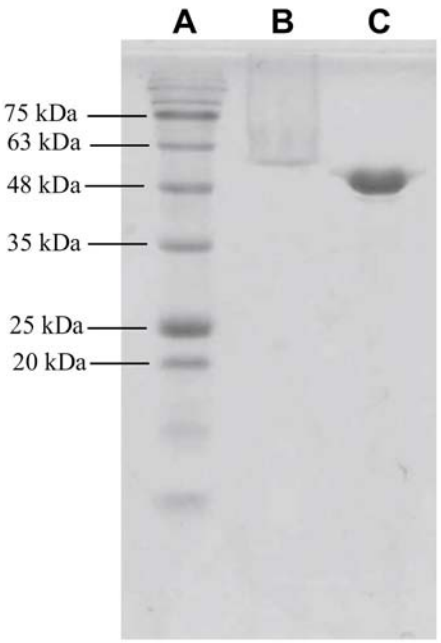

Fig. 2. SDS-Page analysis of NE-JV-1 major capsid protein, revealed with Coomassie staining. **A)** BLUeye Prestained Protein Ladder (2 µL); **B)** Vp54 (4 µL of 1 mg/mL solution; molecular weight of ~53,790 Da); **C)** NE-JV-1 (8 µL of 1 mg/mL solution).

with proteinase K (Sigma P6556) followed by gel filtration chromatography (Bio-Gel P10 eluted with degassed water, d = 1.5 cm, h = 118 cm, flow = 10 ml/h) as described De Castro et al. (2013). Fractions containing the target glycopeptides eluted between 30 and 50% of the total column volume; the yield could not be determined accurately because of the low amounts of protein. Selection of the best sample to measure 2D NMR spectra is described below.

NMR spectroscopy

NMR experiments were recorded in D_2O on a Bruker DRX-600 spectrometer equipped with a cryo-probe and calibrated in acetone (^1H 2.225 ppm, ^{13}C 31.45 ppm), which was used as an internal standard. Routine proton NMR spectra were acquired at 298 K, setting 20 scans, decreasing the residual solvent signal by pre-saturation and fixing the receiver gain at 256. This allowed us to compare the abundance of the carbohydrate component among the five fractions obtained from size exclusion chromatography and to select the most abundant sample (fraction four) to record the full set of 2D NMR spectra.

2DNMR spectra were acquired at 323 K. Homonuclear experiments (TOCSY, T-ROESY and COSY) were recorded using 512 FIDs of 2048 complex data points with 32 scans per FID; a mixing time of 100 and 300 ms was used for TOCSY and T-ROESY spectra acquisition, respectively. ^1H-^{13}C heteronuclear experiments (HSQC, and HMBC) were acquired with 512 FIDs of 2048 complex points with 50 scans for FID for the HSQC and 90 scans for FID for HMBC. Data processing was performed with Bruker Topspin 3.1 program.

Results

Isolation of the main glycopeptide fractions

Proteinase K treatment of the purified major capsid protein and gel filtration chromatography of the glycopeptide mixture (^1H NMR in **Fig. 3a**) resulted in the isolation of several fractions. Each fraction was checked via ^1H NMR spectroscopy, and the first five fractions contained glycopeptides (Fig. 3b–f). These fractions also contained signals arising from

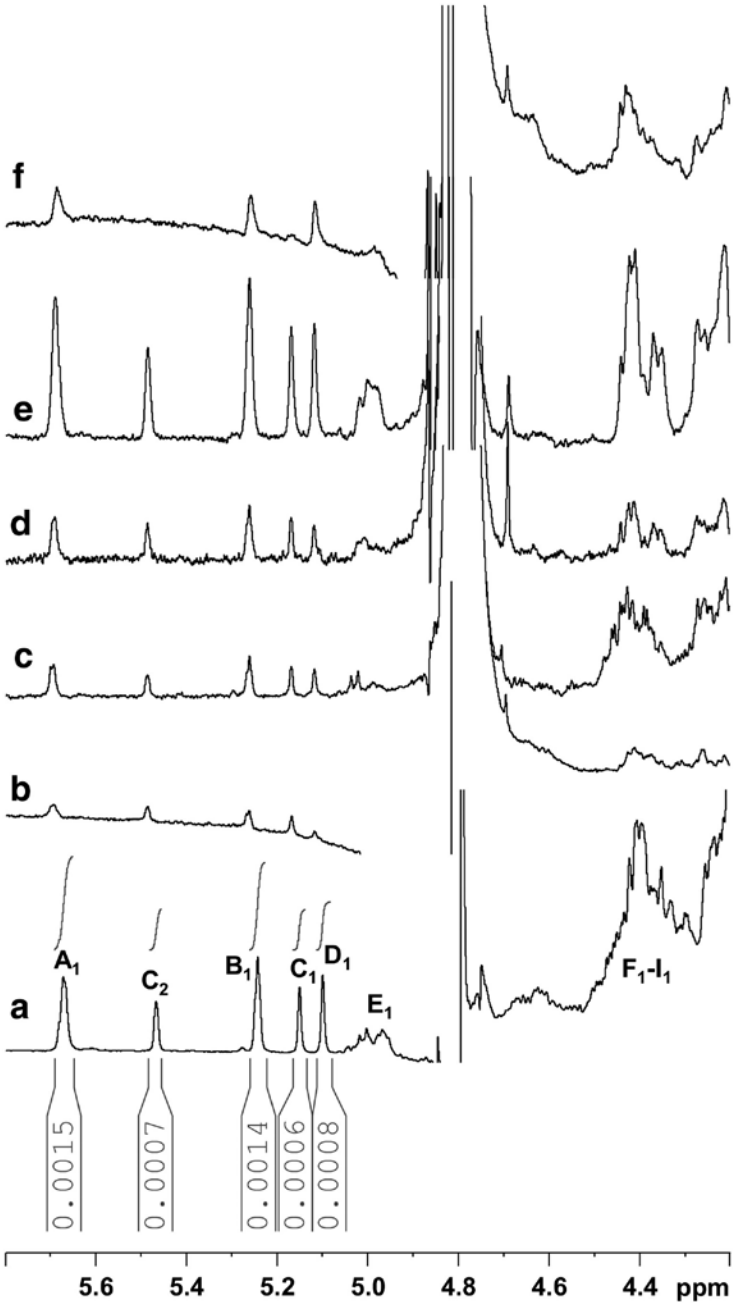

Fig. 3. The (600 Mz, 298 K) proton spectra of **a)** the glycopeptide after enzymatic digestion and prior to purification along with integration of the signals in the anomeric region. **b–f)** The glycopeptides fractions obtained by size exclusion chromatography.

peptide species other than those connected to the glycan; however, no additional purification was attempted due to the low amounts of sample. Preliminary analysis of the proton spectra focused on the region

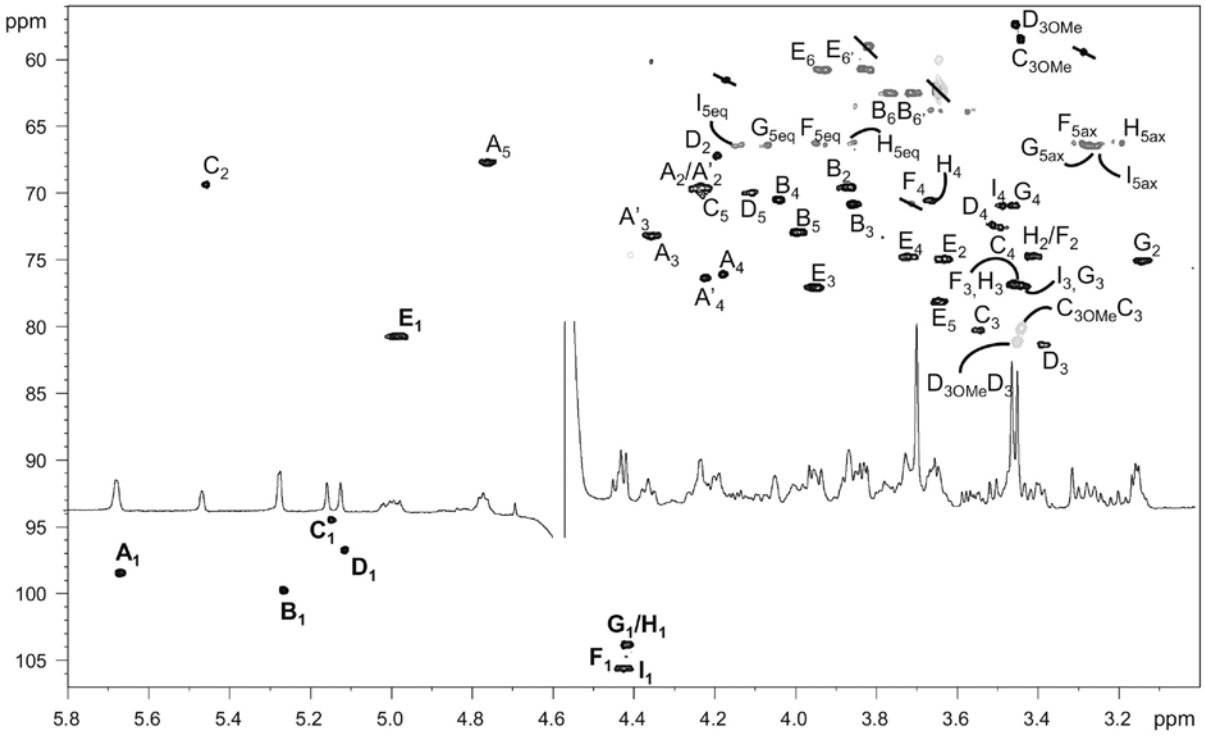

Fig. 4. Superimposition of NE-JV-1 glycopeptide HSQC (*black* and *dark grey*) and HMBC (*pale grey*) spectra at 600 MHz, 323 K. Carbon bearing two hydrogen atoms are colored in *dark grey* because they have densities of opposite sign with respect to the others. Signals crossed are related to the peptide moiety of the glycopeptide.

between 5.7 and 4.9 ppm, because this region is diagnostic of monosaccharide residues α configured at the anomeric center and devoid of signals arising from peptide fragments. Indeed, this region contained several signals with varying intensities depending on the fraction: for instance, the two signals at ca. 5.45 and 5.15 ppm were barely detectable in the last fraction (Fig. 3f). Given the similarity between the different fractions, our analysis was focused on the fourth fraction (Fig. 3e), which had the best spectroscopic signal-to-noise ratio.

NMR determination of the glycopeptide structure(s)

The HSQC spectrum (**Fig. 4**) contained seven anomeric signals, labelled with a letter in order of their decreasing proton chemical shift, a crowded carbinolic region from 4.4 to 3.1 ppm with two O-Me signals (at ca. 3.40 ppm) and several methyl signals at approximately 1.3 ppm, typical of 6-deoxyresidues. Analysis started from **E** which was N-linked to

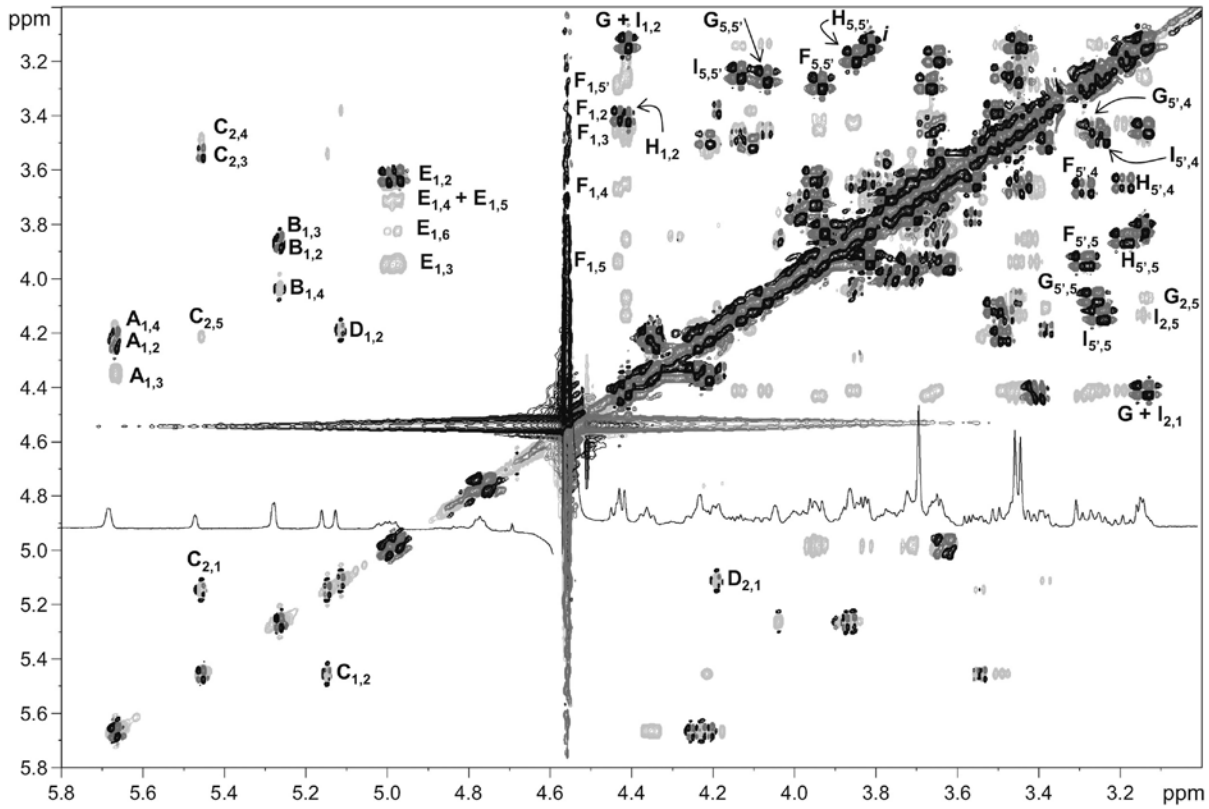

Fig. 5. Superimposition of NE-JV-1 glycopeptide TOCSY (*pale grey*) and COSY (*black* and *dark grey*) spectra at 600 MHz, 323 K.

the protein because of its diagnostic carbon chemical shift (80.7 ppm), while the efficient propagation of magnetization in the TOCSY spectrum (**Fig. 5**) was consistent with the *gluco* stereochemistry of the residue. This information combined with those from the other experiments (COSY, TOCSY and HSQC) identified **E** as a β-glucose substituted at O-3 and O-4, due to the displacement at low field of the respective carbons signals (**Table 1**), similar to what was reported for the analogous residue in the PBCV-1 glycopeptide (De Castro et al. 2013).

Regarding **A**, inspection of the COSY spectrum (Fig. 5) revealed that the signal at 4.67 ppm included signals from two different anomeric protons, each with a distinct correlation to a H-2 signal. Accordingly, the two anomeric signals at 4.67 ppm were labelled **A** and **A′** and for each of them it was possible to trace the proton connectivities up to H-4, beyond which both COSY and TOCSY spectra failed in detecting H-5 as occurs for *galacto* configured residues. In contrast, the T-ROESY experiment (**Fig. 6**) allowed to determine H-5 because connected to H-4 and

Table 1. ^{1}H and ^{13}C chemical shifts (600 MHz) were recorded in D^2O at 310 K, using acetone as internal standard. **C** is acetylated at O-2 (chemical shift $^{1}H/^{13}C$: 2.19/21.6 ppm) and methylated at O-3 ($^{1}H/^{13}C$: 3.44/58.4 ppm). **D** is substituted at position at O-3 with a methyl group ($^{1}H/^{13}C$: 3.45/57.3 ppm)

		1	*2*	*3*	*4*	*5 (5_{eq}; 5_{ax})*	*6; 6′*
A	^{1}H	5.67	4.25	4.35	4.18	4.76	1.33
2,3,4-α-L-Fuc	^{13}C	98.3	69.6	73.1	76.0	67.7	16.3
A′	^{1}H	5.67	4.22	4.36	4.22	4.76	1.33
2,3,4-α-L-Fuc	^{13}C	98.3	69.6	73.1	76.3	67.7	16.3
B	^{1}H	5.26	3.87	3.86	4.04	3.99	3.76; 3.71
α-D-Gal	^{13}C	99.5	69.5	70.8	70.5	72.8	62.5
C	^{1}H	5.15	5.46	3.55	3.49	4.22	1.35
α-L-2OAc,3OMe-Rha	^{13}C	94.4	69.3	80.2	72.5	70.1	18.9
D	^{1}H	5.11	4.19	3.38	3.51	4.11	1.31
α-L-3OMe-Rha	^{13}C	96.7	67.1	81.3	72.4	70.0	18.9
E	^{1}H	4.99	3.63	3.95	3.72	3.64	3.93; 3.82
3,4-β-D-Glc	^{13}C	80.7	74.9	77.0	74.8	78.1	60.8
F	^{1}H	4.44	3.41	3.44	3.67	3.94; 3.29	–
β-D-Xyl	^{13}C	105.6	74.7	76.9	70.5	66.2	–
G	^{1}H	4.42	3.14	3.45	3.46	4.08; 3.27	–
β-D-Xyl	^{13}C	103.8	75.0	76.8	70.9	66.4	–
H	^{1}H	4.42	3.41	3.44	3.661	3.86; 3.19	–
β-D-Xyl	^{13}C	105.6	74.7	76.9	70.5	66.2	–
I	^{1}H	4.42	3.14	3.45	3.49	4.14; 3.26	–
β-D-Xyl	^{13}C	103.8	75.0	76.8	70.9	66.4	–

H-3 via a strong and a medium NOE effect, respectively; in both cases, H-5 was connected to a methyl group. Thus, **A** (or **A′**) was a fucose, α configured at the anomeric center, as inferred from the proton and carbon chemical shift of the anomeric signal (Table 1). Analysis of the carbon chemical shift values indicated that both C-3 and C-4 signals were shifted at low field due to glycosylation; however, even though C-2 had a low carbon chemical shift value (69.6 ppm), the corresponding hydroxyl was glycosylated as deduced by T-ROESY analysis, which detected a correlation between H-2 of **A**, as well as H-2 of **A′**, to H-1 of **B** (Fig. 6).

Indeed, **A** (or **A′**), was a fully substituted α-fucose and its ^{13}C chemical shift values diverged from those of the same residue in PBCV-1 N-glycans (De Castro et al. 2013), a virus in the NC64A group, while they were similar to the values reported for Pbi viruses (CVM-1 and MT325) and SAG viruses (ATCV-1 and TN603) (De Castro et al. 2016). These values support the placement of NE-JV-1 virus in the Pbi group. These three virus groups share the same conserved core oligosaccharide, but differ in the semi-conserved element, which is a L-rhamnose in both SAG and

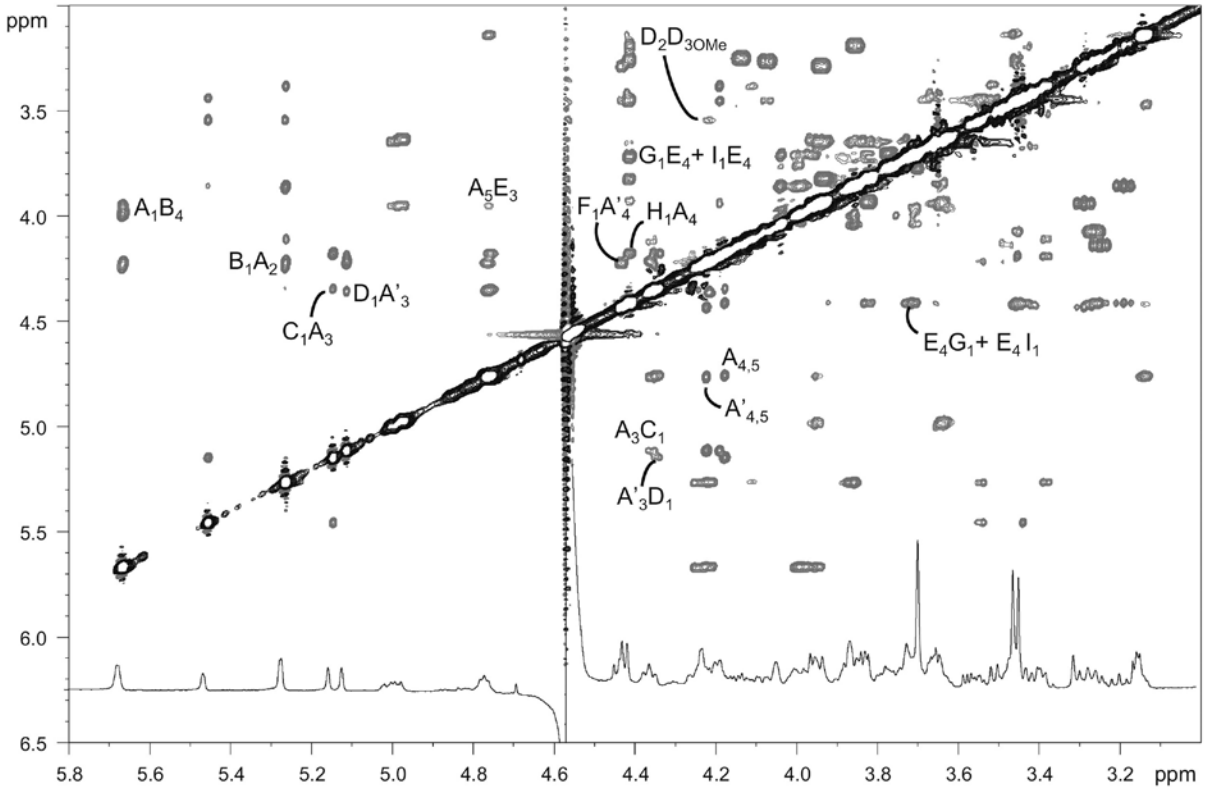

Fig. 6. Expansion of NE-JV-1 glycopeptide T-ROESY spectrum measured at 600 MHz, 323 K.

Pbi viruses, while a D-rhamnose occurs in the NC64A and Syn viruses. Indeed, the carbon chemical shift pattern of **A** (or **A′**) suggested that the nature of the residue at O-3 was a rhamnose with L, and not D, absolute configuration. Last, **A** (or **A′**) was linked at O-3 of **E** as deduced by the pertinent correlation in the T-ROESY spectrum (Fig. 6).

The spectroscopic pattern of **B** residue was comparable to that of **A**, with the difference that H-5 was connected to a hydroxymethylene group instead of a methyl group. Indeed, this unit was a galactose, α configured at the anomeric carbon, not further substituted according to the carbon chemical shift values found, and connected at O-2 of **A** as inferred from the T-ROESY spectrum (Fig. 6).

Regarding the anomeric protons of **C** and **D**, the TOCSY spectrum (Fig. 5) only displayed the correlation with H-2, which instead had correlations with all the other ring protons, including a methyl group, indeed **C** and **D** were two rhamnose units. This information combined with those of the HSQC and HMBC spectra, identified these residues as terminal rhamnose units, α configured at the anomeric center. In

addition, both were methylated at O-3 due to the low field C-3 value (^{13}C of **C**: 80.2 ppm; ^{13}C of **D**: 81.3 ppm), as confirmed by the long-range correlations H-3/C-3_{OMe} and H-3_{OMe}/C-3 in the HMBC spectrum (Fig. 4). Different from **D**, the O-2 position in **C** was acetylated as suggested by the low-field chemical shift of H-2 (5.61 ppm) along with the presence of an acetyl group in the spectrum (^{1}H/^{13}C 2.19/21.5 ppm). The T-ROESY spectrum showed that **C** was connected at O-3 of **A**, while **D** was linked at O-3 of **A′** (Fig. 6).

The HSQC spectrum displayed two anomeric carbon signals at ca. 105 and 103 ppm (Fig. 4), diagnostic of residues β configured at the anomeric center, but the corresponding region in the proton spectrum (ca. 4.42 ppm) had a complex pattern of anomeric signals. Based on our previous experience (De Castro et al. 2016), these signals arise from the βxylose units either proximal or distal to the peptide backbone and their full attribution is possible starting spectra interpretation from the signal of H-5 in axial position (H-5_{ax}) instead of the anomeric proton. Accordingly, COSY spectrum combined with information from HSQC, identified four different H-5ax protons, labelled **F**–**H**, each correlated with the geminal H-5_{eq} proton and to H-4; of note, signals from these protons did not overlap, which enabled the tracing of all correlations up to H-1 (Fig. 5). Thus, two xylose units were identified, one having H-2 density at high field (ca. 4.14 ppm) containing signals from the residues **G** and **I**, and one with H-2 at a lower field (4.41 ppm) with signals from the residues **F** and **H**. The anomeric signal of **F** (4.44 ppm) did not overlap with the others and its carbon chemical shift was at 105.6 ppm; the same value was given to **H** due to the analogies between the proton chemical shifts of the two residues. Accordingly, anomeric carbon chemical shift of **G** and **I** was at 103.8 ppm. Analysis of the T-ROESY spectrum (Fig. 6) established that **F** was linked to O-4 of **A′**,**H** at O-4 of **A**, while **G**, or **I,** was linked at O-4 of **E** (Fig. 6). Thus, **F**, or **H**, occupied the distal position at the conserved core oligosaccharide, while **G**, or **I**, was proximal at the peptide backbone.

Discussion

Phylogenetic analysis of the Pbi chloroviruses identified the Pbi virus NE-JV-1 as a phylogenetic outlier (Jeanniard et al. 2013), leading us to suspect that it might have a unique major capsid protein glycan. Detailed

spectroscopic analyses allowed us to determine the structure of the N-linked glycoforms (Fig. 1b, c) produced by virus NE-JV-1. The structure is similar to the oligosaccharide core of the other chloroviruses with a β-glucose (**E**) N-linked to an asparagine, having a terminal α-xylose (**G** or **I**) at O-4 and a hyperbranched α-fucose (**A**) at position 3, in turn having a terminal α-galactose (**B**) at O-2 and a β-xylose (**F** or **H**) residue at O-4. In addition, the hyperbranched fucose has a L-rhamnose unit substituted at position 3 with a methyl group, a semi-conserved element of the common core oligosaccharide, similar to what was reported for two other Pbi viruses (De Castro et al. 2016). The 3OMe-L-rhamnose can either be acetylated at O-2 (residue **C**, Fig. 1c) or not acetylated (residue **D**, Fig. 1b), and depending on the acetylation status, proton chemical shifts of some other residues are affected as well, e.g., **A** and **A′** or **F** and **I**, resulting in a complex NMR pattern. Finally, the two NE-JV-1 glycoforms are present in almost the same ratio, as indicated by integration of the glycopeptide mixture prior to purification by size exclusion chromatography (Fig. 3a).

Comparison of the NE-JV-1 glycans to those of Pbi chloroviruses CVM-1 and MT325 (Fig. 1d, e) revealed some similarities and some differences. NE-JV-1 did not have any additional monosaccharide added to the core motif as occurs in MT325, which has added either xylulofuranose units or methyl groups (Fig. 1e). Instead, NE-JV-1 presumably encodes an acetyltransferase enzyme that adds an acetyl group at O-2 to the 3OMe-L-rhamnose unit, which also occurs in CVM-1; however, unlike NE-JV-1 the CVM-1 acetylation is rare. This second NE-JV-1 glycoform is also a minor component of SAG chlorovirus ATCV- 1 N-glycans (reported in Fig. 1c, De Castro et al. 2016).

To date, there are two main hypotheses about the role of chloroviruses N-glycans: (i) N-glycans play a key role in the capsid stability, (ii) N-glycans are involved in the host/guest interaction process. Based on the structural data collected so far, the second hypothesis does not seem plausible anymore, indeed viruses belonging to different groups, such as NE-JV-1 and ATCV-1, share the same glycan epitope but have a different host specificity.

Of interest, instead are the results from our ongoing studies on the antigenic variants of the prototype virus, PBCV-1. These antigenic variants present truncated N-glycan structures and are mechanically more fragile compared to the wild type virus, suggesting therefore that N-glycans play a structural role probably contributing to the stability of the capsid.

In this framework, structural elucidation of chloroviruses complex N-glycans will pave the way to new studies, namely which interactions they establish with the underneath protein. All this is now feasible through new emerging approaches (Marchetti et al. 2016), that will increase our understanding about how N-glycans contribute to the stability of the capsid, which in turn is essential to understanding biology of these viruses.

Acknowledgments — Funding for this study was partially provided by the NSF-EPS-CoR Grant EPS-1004094 (JVE), the COBRE program of the National Center for Research Resources Grant P20-RR15535 (JVE), and National Institute for General Medical Science Grant 8P20GM103427 (to G.D.).

References

De Castro C, Molinaro A, Piacente F, Gurnon JR, Sturiale L, Palmigiano A, Lanzetta R, Parrilli M, Garozzo D, Tonetti M, Van Etten JL (2013) Structure of N-linked oligosaccharides attached to chlorovirus PBCV-1 major capsid protein reveals unusual class of complex N-glycans. Proc Natl Acad Sci USA 110:13956–13960. doi:10.1073/pnas.1313005110

De Castro C, Speciale I, Duncan G, Dunigan DD, Agarkova I, Lanzetta R, Sturiale L, Palmigiano A, Garozzo D, Molinaro A, Tonetti M, Van Etten JL (2016) N-linked glycans of chloroviruses sharing a core architecture without precedent. Angew Chem Int Ed 55:654–658. doi:10.1002/anie.201509150

Doms RW, Lamb RA, Rose JK, Helenius A (1993) Folding and assembly of viral membrane proteins. Virology 193:545–562 Jeanniard A, Dunigan DD, Gurnon JR, Agarkova IV, Kang M, Vitek J, Duncan G, McClung OW, Larsen M, Claverie J-M, Van Etten JL, Blanc G (2013) Towards defining the chloroviruses: a genomic journey through a genus of large DNA viruses. BMC Genom 14:158

Marchetti R, Perez S, Arda A, Imberty A, Jiménez-Barbero J, Silipo A, Molinaro A (2016) ''Rules of Engagement'' of protein-glycoconjugate interactions: a molecular view achievable by using NMR spectroscopy and molecular modeling. Chemistry Open 5(4):274–296. doi:10.1002/open.201600024

Olofsson S, Hansen JES (1998) Host cell glycosylation of viral glycoproteins—a battlefield for host defense and viral resistance. Scand J Infect Dis 30:435–440

Quispe CF, Esmael A, Sonderman O, McQuinn M, Agarkova I, Battah M, Duncan GA, Dunigan DD, Smith TPL, De Castro C, Speciale I, Ma F, Van Etten JL (2016) Characterization of a new chlorovirus type with permissive and non-permissive features on phylogenetically related algal strains. Virology 500:103–113

Van Etten JL, Dunigan DD (2012) Chloroviruses: not yet everyday plant virus. Trends Plant Sci 17:1–8

Van Etten JL, Dunigan DD (2016) Giant chloroviruses: five easy questions. PLoS Pathog 12:e1005751. doi:10.1371/journal.ppat.1005751

Van Etten JL, Gurnon JR, Yanai-Balser GM, Dunigan DD, Graves MV (2010) Chlorella viruses encode most, if not all, of the machinery to glycosylate their glycoproteins independent of the endoplasmic reticulum and Golgi. Biochem Biophys Acta 1800:152–159

Vigerust DL, Shepherd VL (2007) Virus glycosylation: role in virulence and immune interactions. Trends Microbiol 15:211–218

Yamada T, Onimatsu H, Van Etten JL (2006) *Chlorella* viruses. Adv Virus Res 66:293–336